

Significance of GPR polarisation for improving target detection and characterisation

Maurizio Lualdi* and Federico Lombardi¹

Department of Civil and Environmental Engineering, Politecnico di Milano, Piazza Leonardo da Vinci, 32, Milan 20133, Italy

(Received 30 October 2013; accepted 25 July 2014)

1. Introduction

Ground penetrating radar (GPR) is a non-destructive geophysical technique that uses high-frequency electromagnetic (EM) waves for imaging the shallower layers of the earth.[1] In civil engineering, the method has been successfully applied in concrete high-rise inspection,[2–6] masonry and cultural heritage,[7–11] and environmental investigations. [12–14] The widespread diffusion of GPR is due to its high-resolution imaging capability and survey time effectiveness, along with the possibility of providing a three-dimensional (3D) model of the site, in which a number of closely spaced bidimensional scans are connected in a predefined sequence. This procedure has the advantage of looking at the entire survey site at once with the possibility of following a target out of the two-dimensional (2D) domain feature that becomes very significant in areas with multiple intersecting or dipping targets (pipes and rebar) that may be hard to identify on single-radar profiles.[15] To guarantee a correct reconstruction and avoid spatial aliasing problems, the acquired grid of traces must be sufficiently dense and regular to fulfil the signal spatial sampling constraints.[16] Having been an unemployed strategy (or just approximated through sparsely bidimensional profiles) for a long time, with the increasing computing capability and hardware development, the 3D surveys are becoming an established acquisition methodology. Following this direction, multi-channel GPR equipment and data are being regularly employed especially for large area surveys.

* Corresponding author. Email: maurizio.lualdi@polimi.it

However, the 3D reconstruction performance can be corrupted when acquiring across targets that show some directional features: in this case the mixture of all scattering phenomena, mainly target depolarisation, significantly impact on the backscattered EM wavefield and must be taken into account.[17] Depolarisation is an effect of scattering that modifies the plane of propagation of the returning wavefield that will be collected at the receiver antenna of the GPR equipment, commonly dipole antennas that show a strictly directional radiation pattern: transmitting dipole emits a linearly polarised wave whose electric field vibrates along the long axis of the antenna, and thus, for reciprocity theorem, the receiver is sensible only to the components parallel to its longest dimension.[18] This means that targets that affect propagation features can be even missed if the geometry of the survey is adverse or its properties are such that huge modifications are induced on the scattered wavefield.[19]

Other class of possible GPR targets is the point scatterer, which radiates uniformly through the 3D space (Mie scattering) and does not cause any polarisation plane deviation or other influential variation. Ideally, in this case, a complete miss is not possible.

These two antithetical behaviours, representing the signatures of the most common georadar targets in civil engineering applications, indicate that detection or avoidance of a specific target can be managed through its polarimetric response. This provides the GPR technique with an opportunity for producing improved images of objects in the subsurface, together with the possibility of planning an effective survey.

This paper provides an insight of the effect of GPR polarisation features applied on building inspection. We exploit the advantages brought by changing dipoles mutual orientation to increase the knowledge and characterisation of geometrically complex environment in which single dipole configuration can be inadequate. With two field examples, we show how a multicomponent can efficiently discriminate between different classes of targets and can be suitable for giving evidence only to a certain kind of scatterer at once, providing a clearer and more accurate image of the subsurface features.

2. GPR polarisation and antenna configurations

To determine quantitatively correct GPR images, it is necessary to account for the antenna radiation patterns, the vectorial nature of EM wavefield propagation and the characteristics of the subsurface scatterers.

As briefly described, the dipole antennas have a strong directionality radiation that implies significant variations in the amount of collected energy in the case of misalignment between the transmitter and the receiver. Under the assumption of homogeneous soil (neglecting medium depolarisation and dispersion effects), point heterogeneities in the subsurface can be represented by infinitesimal dipoles with moments parallel and proportional to the incident georadar wavefields. In the case of elongated objects, the target is approximately a dipole antenna with equal geometrical characteristics. Therefore, maximum pickup will result when the receiver antenna is oriented as the primary geometrical dimension of the scatterer.[20]

The boundary situation, commonly called a polarisation mismatch, occurs when the receiver antenna is rotated orthogonal to the transmitter one, as ideally the energy collected by the dipole is close to zero.

Conventional GPR surveys use parallel co-polarised configurations, solution that ensures adequate detection performance employing convenient hardware design. Transmitter and receiver can be arranged to each other to obtain different GPR configurations (also referred as components), displayed in [Figure 1](#).

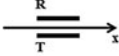


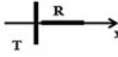
	CO-POLARIZED	CROSS-POLARIZED
PARALLEL		
PERPENDICULAR		

Figure 1. Sketch representation of the different transmitter–receiver configurations. **T** is the transmitter and **R** the receiver dipole. Line of data acquisition is indicated and always points to the right side of the figure.

Distinctions are made considering:

- mutual orientation: co-polarised (dipoles parallel to each other) and cross-polarised (dipoles mutually orthogonal);
- line of data collection: parallel (transmitter held along the moving direction) and perpendicular (transmitter orthogonal to it).

Because each antenna arrangement is sensitive towards different features of the received wavefield, a transmitter/receiver polarisation mismatch or adverse target geometry does not always mean a lower informative result.

Although cross-polarised data generally have much lower amplitudes than co-polarised data, they may contain significant information. Cross-pole antennas are commonly employed to reduce clutter and ring-down effect and to improve antenna isolation.[21–23] These components have also been included in migration algorithms to enhance target lateral resolution and provide better imaging results.[24–27] Targets are visible using cross-configuration when they scatter electric field component orthogonal to the one radiated by the transmitter antenna, a situation commonly encountered with rough surfaces and small spherical objects. This configuration could be unable to detect targets that show some directionality, as they scattered preferentially in a precise direction and do not introduce additional components in the scattered wavefield. Therefore, considering the scattering assumption, elongated cylindrical shape target are best imaged using mutually parallel dipoles, although with some significant remarks: metallic pipes yield strong reflections when oriented parallel to the long axis of a dipole transmit antenna, while high-impedance dielectric pipes better scatter incident wave when the incident polarisation is perpendicular to the long axis of the pipe.[28–30]

Examples of remarkable application of multicomponent GPR technique and polarimetric analysis are the field of mine/Unexploded ordnance (UXO) detection, [31,32] civil engineering [33,34] and geology.[35]

3. Experimental campaigns

To address the polarisation phenomena and demonstrate how these can provide further information on the acquired area, two multicomponent GPR surveys (for definitions and naming convention, refer Figure 1) have been carried out: a first methodological 2D analysis of the polarisation impact on rebar detection (Section 3.1) and a 3D analysis in

which a mixture of elongated targets and point scatterers clearly proves the potential of multicomponent acquisition (Section 3.2).

The two experiments were recorded using an Ingegneria dei Sistemi Aladdin (IDS-Aladdin, Italy, [Figure 2\(a\)](#)) georadar system, which consists in two couples of highly balanced dipole antennas ([Figure 2\(b\)](#)). The central frequency of the antenna is 2 GHz, with an offset of 6 cm for both couples. This configuration guarantees precise matching between the common midpoints (CMPs) [36] of each possible antenna configuration, as the antennas are not moved away from the line of data collection. In addition, the design permits orthogonally polarised scans to be acquired in a single pass, meaning that the transmitting antenna for each couple of co- and cross-polarised scans does not change.

Accurate profile correspondence and spacing was obtained through the Pad System for Georadar (PSG, US Patent no. US 7,199,748 B2 of Politecnico di Milano, Italy, [37] and [Figure 2\(a\)](#)), a pad whose surface is modelled with parallel tracks that are few millimetres high. The GPR antenna is dragged along the tracks so that parallel and regularly spaced profiles are rapidly executed and unchanging antenna orientation is warranted.

Data were processed using a tool developed by Politecnico di Milano running on Mathworks/MATLAB software.

3.1 Survey 1: polarisation impact on linear metallic target

First survey was carried out over a concrete block in which three metallic rods with diameters of 16, 10 and 6 mm and spaced approximately 30 cm were buried ([Figure 3\(a\)](#)). The three diameters represent commonly employed reinforcement dimension for the principal civil engineering structures, from bridges and dams down to housing structures.

The same profile has been acquired 10 times for each dipoles configuration (co-pole and cross-pole) with an angular sampling of 10° starting with transmitting dipole oriented perpendicular to the survey direction. Angular rotation was performed through a plate mounted on a protractor ([Figure 3\(b\),\(c\)](#)). The selected angular step represents the finer sampling that can provide consistent results considering the accuracy and precision of the described mechanical system.

The dual polarised design of the GPR system permits to simultaneously acquire data from 0° to 180° with a 90° rotation only. The first set of orientation (from 0° to 90°) belongs to one pair of dipoles (grey-shaded area in [Figure 2\(b\)](#), perpendicular configuration), while the angles from 100° to 180° to the orthogonal one (black-shaded area in [Figure 2\(b\)](#), parallel configuration).

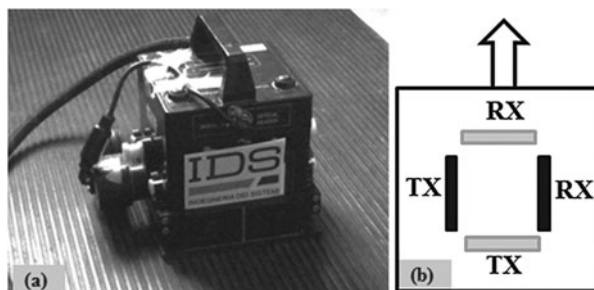


Figure 2. IDS-Aladdin georadar equipment. (a) Georadar and PSG device. (b) Dipoles scheme and geometry.

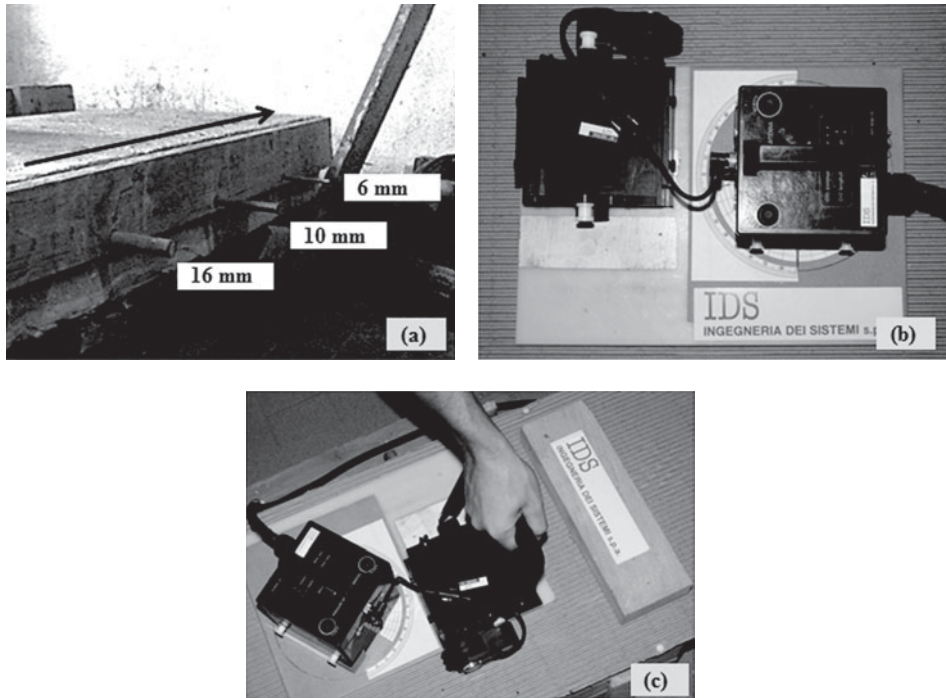


Figure 3. Survey 1 details. (a) Side view of the concrete block with buried steel bar (measures are in millimetres), the black arrow indicates the acquisition direction. (b, c) Georadar antenna, PSG and protractor device.

Co-pole configuration results and a sketch of the target to simplify text recalling are shown in [Figure 4](#).

Imaging of linear metallic target is hugely conditioned by alignment mismatch between object and GPR antennas, and its severity grows inversely proportional to the bar diameter. Considering that for metallic target the maximum response occur in parallel co-pole configuration with dipoles aligned with the longest axis of the pipe, the orientation that makes the perpendicular co-pole response a maximum also makes the perpendicular a minimum ([Figure 4](#), 0° and 90° frames, respectively). Globally, variations in the hyperbola imaging are noticeable when they differ by more than 30° .

Two substantial trends can be highlighted:

- The larger rods (particularly target marked 1 in [Figure 4](#)) are visible at all angles, also when there is a complete polarisation mismatch, i.e. approaching 90° orientation; however, their energy is strongly reduced leading to the risk of object missing in the case of less homogeneous soil or deeper location. Compared with the optimal alignment (0° - and 180° -oriented frames), the thickness of the hyperbola is lower and the shape is just outlined.
- Thinner bar (target 3 in [Figure 4](#)) is hugely affected by deviations from the optimal survey geometry. While its corresponding diffraction hyperbolas are visible up to $\sim 50^\circ$ and again from 140° , they are significantly attenuated in the range of 60° – 130° . When the dipole is approaching a 90° rotation, the rebar signature vanishes, until it becomes not even detectable by the receiver antenna.

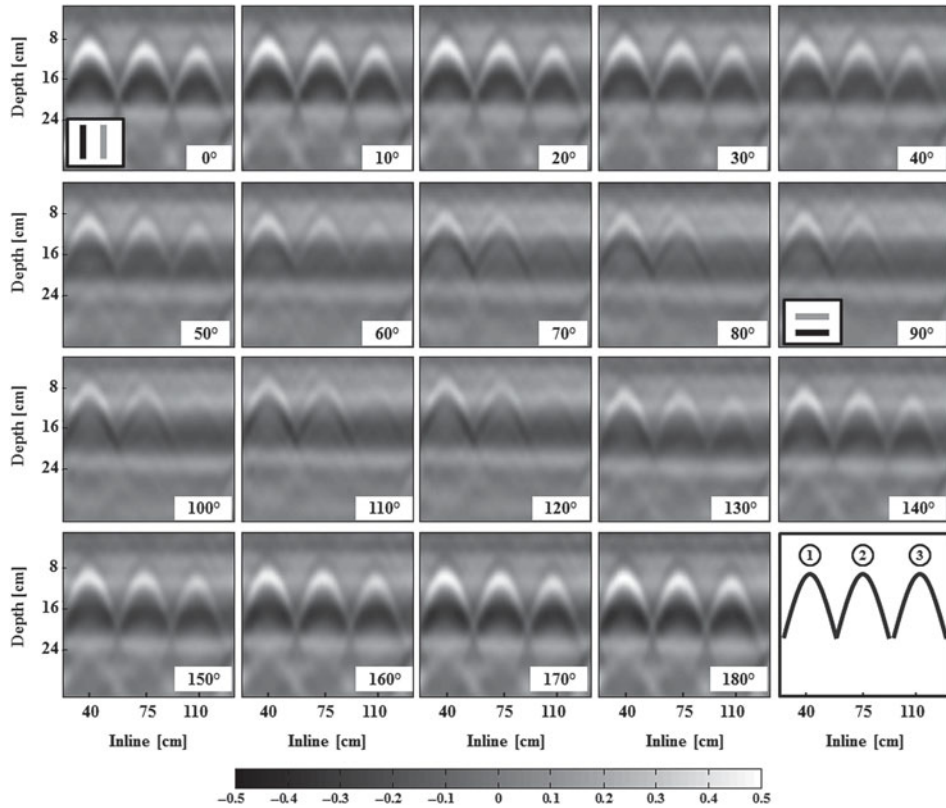


Figure 4. Survey 1 results. Co-pole data, profiles orientation and relative dipoles position are inserted in each frame. All the profiles are plotted using equal amplitude scale and contrast settings.

The same acquisition procedure has been applied for the cross-polarised survey, whose results are presented in [Figure 5](#).

Despite a similar behaviour in terms of angular drifting sensibility, in this case the trend of the target signatures is totally antithetical to the co-pole results: alignment between the bar and the transmitter antenna (corresponding to the state of maximum target scattering) or the receiver antenna (condition of maximum pick up) produces a radargram in which the collected energy is close to zero, as there is a complete polarisation mismatch. The overall reduction in the collected energy is evident considering the following:

- The larger rod (target 1 in [Figure 5](#)) vanishes in disagreement with its behaviour in polarisation mismatch with co-pole configuration (90° frame of [Figure 4](#)).
- The maximum of the cross-pole configuration (40°/50° and 130°/140° frame in [Figure 5](#)) should be very similar to the corresponding co-pole frames, as a consequence of the symmetrical response of target scattering.[38]

These considerations are highlighted in [Figure 6](#).

This experiment demonstrates that when dealing with thin elongated targets, a single-component acquisition could be significantly inadequate because of the high risk of failure in target detection, underlining the need of a multi-polarisation approach. A proof that the cross-pole configuration can efficiently get around scattering from elongated target, improving the imaging of the closest areas of the subsurface, is clearly described.

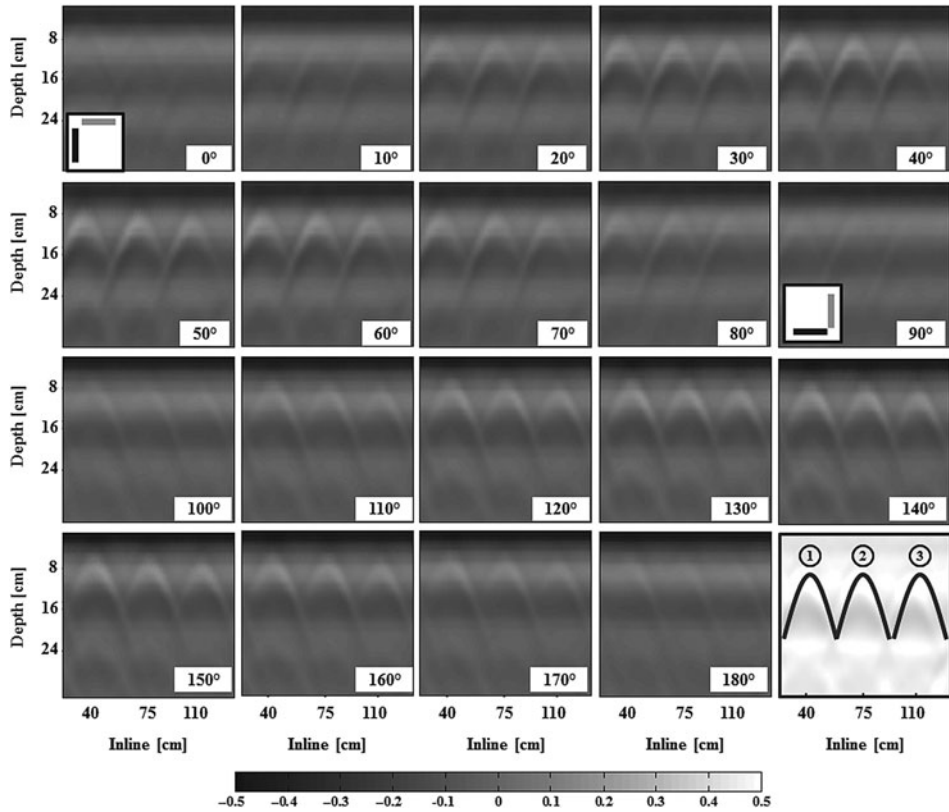


Figure 5. Survey 1 results. Cross-pole data, profiles orientation and relative dipoles position are inserted in each frame. All the profiles are plotted using equal amplitude scale and contrast settings.

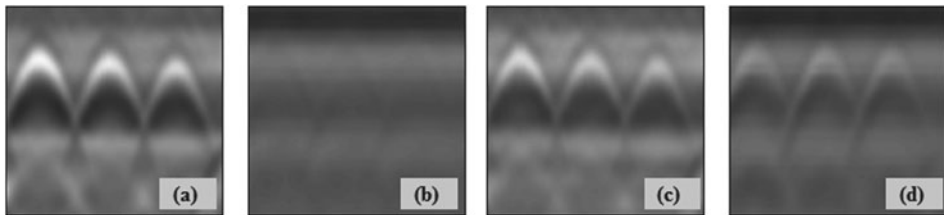


Figure 6. Survey 1, comparison of the polarisation effects. Optimum alignment condition for (a) co-pole and (b) cross-pole configurations. Half-space rotation for (c) co-pole and (d) cross-pole configurations.

3.2 Survey 2: multicomponent for target characterisation

A second experiment has been performed to show the discriminant capability of the combined use of co-pole and cross-pole configurations.

A multicomponent 3D GPR data volume was acquired over a buried heating coil composed of a complex mesh of water-filled thin pipes laid at accurate and consistent spacing in a plastic tray (Figure 7(a), details of the tray in Figure 7(b)). The picture shows the presence of pipes of different length, orientation and path.

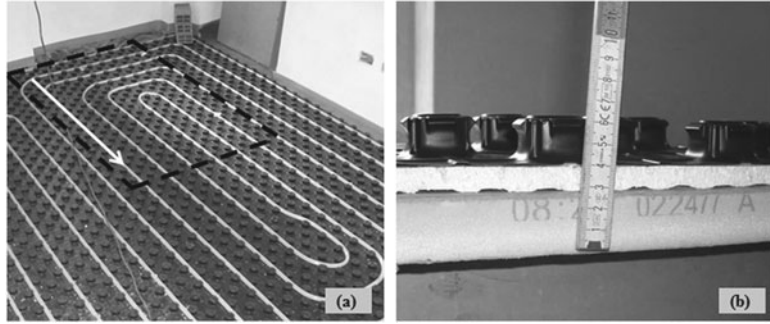


Figure 7. Survey 2 details. (a) Heating system and coil layout. Dashed area represents the PSG position; the white arrow indicates acquisition geometry and first profile. (b) Zoom of the plastic tray that casts the pipes. Measures are in centimetres.

Through a four-channel control unit, all the four components of [Figure 1](#) have been collected at the same time with the aid of the PSG (dashed border in [Figure 7\(a\)](#), the white arrow represents survey geometry and first acquired profile). Profiles spacing was of 0.8 cm and a total of 117 profiles were collected (processing sequence detailed in [Table 1](#)).

Time slices from each component are presented in [Figure \(8\)](#).

Just from a first view, one can clearly see the effect of polarisation: pipes are evident with the co-pole configurations (perpendicular in [Figure 8\(a\)](#) and parallel in [Figure 8\(b\)](#)) depending on their orientation, while the crossed components (perpendicular in [Figure 8\(c\)](#) and parallel in [Figure 8\(d\)](#)) completely eliminate their signatures providing only the turning strokes of the pipes. Results are in agreement with those obtained in [Figure 5](#): mutually orthogonal dipoles are able to image the pipe only when its orientation is in the $40^\circ - 70^\circ$ range, the orientation interval which corresponds to the minimum energetic level for the co-pole configuration ([Figure 4](#)). Antithetically, when the pipe reaches lower or higher inclination, the co-pole configuration is able to collect the most of the backscattered energy, while a complete polarisation mismatch occurs when transmitter and receiver are orthogonal.

Furthermore, looking at all four time slices as a group ([Figure 9](#)), they clearly appear to provide complementary views of the acquired area and giving evidence to a precise target depending on its polarimetric behaviour:

- Co-pole components emphasise pipes but lose precise definition in the case of non-straight paths and resolution for possible closely spaced objects.
- Cross-pole components miss targets that show consistent directionality features but accurately image curved stroke and avoid effects of strong scattering that can mask the nearest part of a pipe.

The situation demonstrates that a single-component acquisition is not able to deliver a complete representation of the area, as each of the four configurations (even if the two crossed are degenerated thus closely identical) loses some features. Energy reduction is

Table 1. Processing steps and algorithm details.

<i>Time calibration</i>	<i>Trace alignment</i>	<i>Frequency filtering</i>
Time shift	Correlation window	Zero-phase Butterworth filter

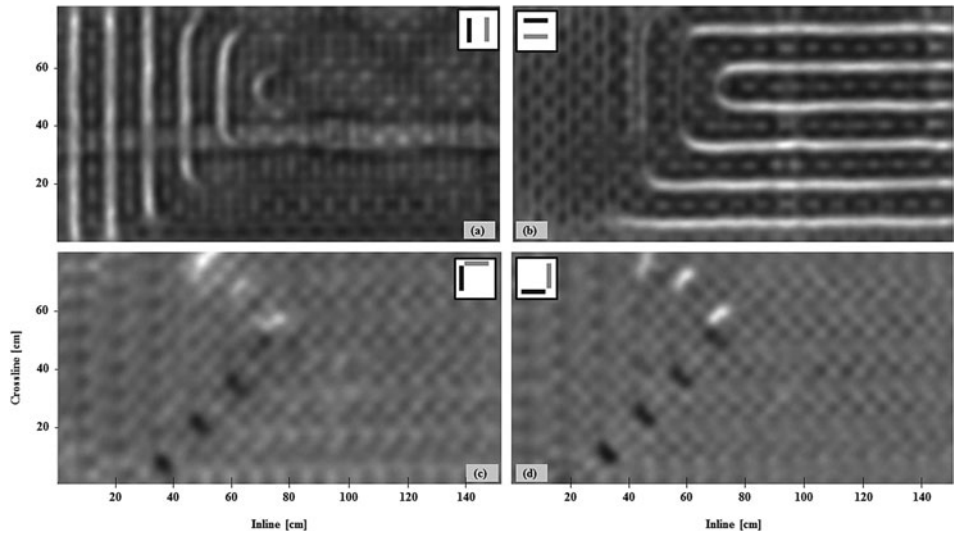


Figure 8. Survey 2 time slice. Time 0.7 ns. (a) Co-pole perpendicular configuration. (b) Co-pole parallel configuration. (c) Cross-pole perpendicular configuration. (d) Cross-pole parallel configuration.

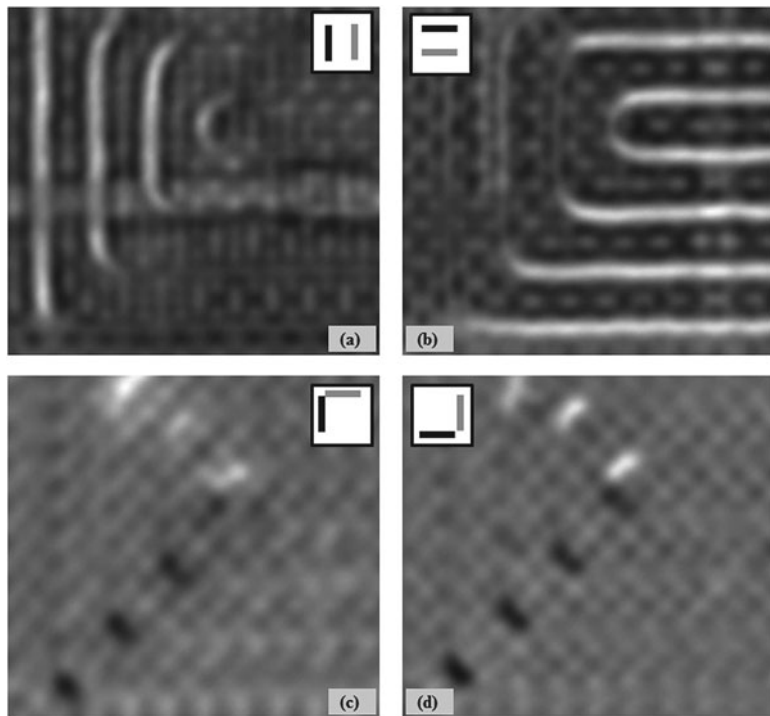


Figure 9. Survey 2, focus on the polarisation effects. Co-pole (a) perpendicular and (b) parallel, cross-pole (c) parallel and (d) perpendicular configurations.

visible if one compares the imaging of pipes-free areas of the acquired pad: some elements in the cross-pole time slices are wrongly joined, with a loss of resolution, but they can still be counted and properly sketched.

In this case, cross-configuration can efficiently overcome the pipes mesh and image the plastic tray, a structure that is mostly masked by the scattering of the pipes when using parallel or perpendicular co-pole configurations.

4. Conclusions

Focusing on high-frequency GPR equipment for civil diagnosis application, this paper analyses the impact of wave polarisation and antenna geometry providing an insight into the benefits of considering and having this information available. Even if polarisation properties of GPR signal are seldom considered during data analysis and post-processing, they could bring significant benefits, especially for:

- optimisation: knowing the depolarisation properties of targets can aid to project a time-saving and effective GPR survey;
- discrimination: the physical shape and composition of targets will influence the polarisation of the scattered field, and this enables cross-pole and co-pole antenna configurations to discriminate between different classes of targets;
- identification: combining the information on the possible target and its polarimetric response, detected target can be correctly recognised and classified.

Two field examples sustain the validity and efficacy of a multicomponent approach to ensure that all significant information is captured by the survey. We extend the application of crossed dipoles not only for improving antennas performances but also when the scope is to highlight features that may be masked by the scattering of elongated targets in traditional co-pole configurations.

The importance of considering the use of cross-pole data in addition to traditionally acquired co-pole data when GPR is used in civil engineering where it is easy to find a mixture between elongated targets and point scatterers has clearly been demonstrated through this study. Furthermore, the method could be a useful tool for seismic structural assessment.[39,40]

Acknowledgements

The authors are thankful to IDS Company for the supply of georadar equipment.

References

- [1] Daniels DJ. Ground penetrating radar. London: Peter Peregrinus Ltd; 2004.
- [2] Hugenschmidt J, Mastrangelo R. GPR inspection of concrete bridges. *Cement Concrete Comp.* 2006;28:384–392.
- [3] Sgambi L, Gkoumas K, Bontempi F. Genetic algorithm optimization of precast hollow core slabs. *Comput Concrete.* 2014;13(3):389–409.
- [4] Garavaglia E, Pizzigoni A, Sgambi L, Basso N. Collapse behaviour in reciprocal space frame structures. *Struct Eng Mech.* 2014;46(4):533–547.

- [5] Xu X, Zeng Q, Li D, Wu J, Wu X, Shen J. GPR detection of several common subsurface voids inside dikes and dams. *Eng Geol.* 2010;111:31–42.
- [6] Annan AP, Cosway SW, DeSouza T. Application of GPR to map concrete to delineate embedded structural elements and defects. *Proceedings of 9th International Conference on Ground Penetrating Radar; 2002 April 29–May 2; Santa Barbara, CA (USA); 2002.*
- [7] Binda L, Cantini L, Lualdi M, Tedeschi C, Saisi A, Zanzi L. Investigation on structures and materials of the Castle of Avio (Trento, Italy). *Adv Archit.* 2005;20:599–610.
- [8] Binda L, Lualdi M, Saisi A, Zanzi L. Radar investigation as a complementary tool for the diagnosis of historic masonry buildings. *Int J Mater Struct Integrity.* 2011;5:1–25.
- [9] Binda L, Lualdi M, Saisi A. Investigation strategies for the diagnosis of historic structures: on-site tests on Avio Castle, Italy and Pišcece Castle, Slovenia. *Can J Civil Eng.* 2008;35:555–566.
- [10] Binda L, Zanzi L, Lualdi M, Condoleo P. The use of georadar to assess damage to a Masonry Bell Tower in Cremona Italy. *NDT&E Int.* 2004;38:171–179.
- [11] Lualdi M, Zanzi L. GPR investigations to reconstruct the geometry of the wooden structures in historical buildings. *Proceedings of 9th International Conference on Ground Penetrating Radar; 2002 April 29–May 2; Santa Barbara, CA (USA); 2002.*
- [12] Lualdi M, Zanzi L, Sosio G. A 3D GPR survey methodology for archaeological applications. *Proceedings of 11th International Conference on Ground Penetrating Radar; 2006 June 19–22; Columbus, OH (USA); 2006.*
- [13] Lualdi M, Zanzi L. 2D and 3D experiments to explore the potential benefit of GPR investigations in planning the mining activity of a limestone quarry. *Proceedings of 10th International Conference on Ground Penetrating Radar; 2004 June 21–24; Delft, NL; 2004.*
- [14] Lualdi M, Zanzi L. Testing a safe acquisition procedure for an effective application of GPR to security operations. *Proceedings of 11th Symposium on the Application of Geophysics to Engineering and Environmental Problems; 2005 April 3–7; Atlanta, GA; 2005.*
- [15] Bernstein R, Oristaglio M, Miller DE, Haldorsen J. Imaging radar maps underground objects in 3-D. *IEEE Comput Appl Power.* 2000;13:20–24.
- [16] Lualdi M, Binda L, Zanzi L. Acquisition and processing requirements for high quality 3D reconstructions from GPR investigations. *Proceedings of International Symposium on Non Destructive Testing in Civil Engineering; 2003 September 16–19; NDT-C, Berlin, DE; 2003.*
- [17] Daniels DJ, Wielopolski L, Radzevicius SJ, Bookshar J. 3D GPR polarization analysis for imaging complex objects. *Proceedings of 16th EEGS Symposium on the Application of Geophysics to Engineering and Environmental Problems; 2003 April 6–10; San Antonio, TX (USA); 2003.*
- [18] Balanis CA. *Antenna theory: analysis and design.* New York (NY): Wiley; 1982.
- [19] Beckmann P. *The depolarization of electromagnetic waves. Vol. 1.* Boulder: Golem Press; 1968.
- [20] Balanis CA. *Advanced engineering electromagnetics.* New York (NY): Wiley; 1989.
- [21] Guy ED, Daniels JJ, Radzevicius SJ. Demonstration of using crossed dipole GPR antennae for site characterization. *Geophys Res Lett.* 1999; 26: 3421–3424.
- [22] Radzevicius SJ, Guy ED, Daniels JJ, Vendl MA. Significance of crossed-dipole antennas for high noise environments. *Proceedings of Symposium on the Application of Geophysics to Environmental and Engineering Problems; 2000 February 20–24; Denver, CO (USA); 2000.*
- [23] Radzevicius SJ, Guy ED, Daniels JJ. Pitfalls in GPR data interpretation: differentiating stratigraphy and buried objects from periodic antenna and target effects. *Geophys Res Lett.* 2000;27:3393–3396.
- [24] Streich R, Van der Kruk J. Accurate imaging of multicomponent GPR data based on exact radiation patterns. *IEEE Trans Geosci Remote Sens.* 2007;45:93–103.
- [25] Van der Kruk J, Zeeman JH, Groenenboom J. Multicomponent imaging of different objects with different strike orientation. *Proceedings of 9th International Conference on Ground Penetrating Radar; 2002 April 29–May 2; Santa Barbara, CA (USA); 2002.*
- [26] Böniger U, Tronicke J. Subsurface utility extraction and characterization: combining GPR symmetry and polarization attributes. *IEEE Trans Geosci Remote Sens.* 2012;50:736–746.
- [27] Van der Kruk J, Wapenaar CPA, Fokkema JT, Van den Berg PM. Three-dimensional imaging of multicomponent ground penetrating radar data. *Geophysics.* 2003;68:1241–1254.
- [28] Radzevicius SJ, Daniels DJ. Ground penetrating radar polarization and scattering from cylinders. *J Appl Geophys.* 2000;45:111–125.

- [29] Roberts RL, Daniels JJ. Analysis of GPR polarization phenomena. *J Environ Eng Geophys.* 1996;1:139–157.
- [30] Roberts RL. Analysis of theoretical modeling of GPR polarization phenomena [dissertation]. Columbus (OH): The Ohio State University; 1994.
- [31] Chen CC, Higgins MB, O’Neill K, Detsch R. Ultrawide-bandwidth fully-polarimetric ground penetrating radar classification of subsurface unexploded ordnance. *IEEE Trans Geosci Remote Sens.* 2001;39:1221–1230.
- [32] Hyoung-sun Y, Evans M, Kobashigawa J, Iskander M. Advanced classification of UXO using fully polarimetric GPR and frequency-polarization features. *Geoscience and Remote Sensing Symposium (IGARSS); 2010 July 25–30; Honolulu, HI (USA); 2010.*
- [33] Lualdi M, Lombardi F. Orthogonal polarization approach for three dimensional georadar surveys. *NDT&E Int.* 2013;60:87–99.
- [34] O’Neill K, Lussky RF Jr, Paulsen KD. Scattering from a metallic object embedded near the randomly rough surface of a lossy dielectric. *IEEE Trans Geosci Remote Sens.* 1996;34(2):367–376.
- [35] Tsoflias GP, Van Gestel JP, Stoffa PL, Blankenship DD, Sen M. Vertical fracture detection by exploiting the polarization properties of ground-penetrating radar signals. *Geophysics.* 2004;69:803–810.
- [36] Yilmaz O. *Seismic data analysis.* Tulsa: Society of Exploration Geophysicists; 2001.
- [37] Lualdi M. True 3D acquisition using GPR over small areas: A cost effective solution. *Proceedings of 16th Symposium on the Application of Geophysics to Engineering and Environmental Problems; 2011 April 10–14; Charleston, SC (USA); 2011.*
- [38] Villela A, Romo JM. Invariant properties and rotation transformations of the GPR scattering matrix. *J Appl Geophys.* 2013;90:71–81.
- [39] Valente M. Seismic performance assessment of a non-ductile RC building retrofitted by steel bracing or fiber-reinforced polymers. *Appl Mech Mater.* 2012;234:84–89.
- [40] Valente M. Seismic strengthening of non-ductile R/C structures using infill wall or ductile steel bracing. *Adv Mater Res.* 2013;602-604:1583–1587.